Sādhanā (2020) 45:27
https://doi.org/10.1007/s12046-019-1252-4

Corrosion behavior of reinforcing bar in magnesium phosphate cement based on polarization curve

LI JUN[1,2,3,4,*], JI YONGSHENG[2] and XU ZHISHAN[2]

[1]School of Civil Engineering and Architecture, Kaifeng University, Henan Kaifeng 475004, China
[2]State Key Laboratory for Geomechanics and Deep Underground Engineering, China University of Mining and Technology, Xuzhou 221008, Jiangsu, China
[3]Sponge City Engineering Materials Technology Research center of Kaifeng, Henan Kaifeng 475004, China
[4]Collaborative Innovation Center for New Energy-Saving Building Materials of Kaifeng University, Henan Kaifeng 475004, China
e-mail: l1979394@163.com

MS received 26 January 2019; revised 20 August 2019; accepted 16 October 2019

Abstract. Apart from focusing on the analysis of the characteristics of reinforcing bars during corrosion, such as open circuit potential and polarization, the study also engages in the investigation of their corrosion in magnesium phosphate cement (MPC). For a more comprehensive understanding of the rusting performances, a comparison was made by an electrochemical workstation between the reinforcing bars in the MPC system and in the ordinary cement. Meanwhile, under an optical microscope, an observation was conducted on the corrosion morphology in MPC at different ages of concrete while during MPC hydration, an exploration based on pH changes and polarization curve theory was carried out to learn about the mechanism of the resistance of the reinforcing bars in MPC to corrosion. Despite their extremely slow rate, corrosion behaviors were practically found in the reinforcing bars in MPC. Both the changes in pH and the formation of ammonium phosphate metal complex in the weak base were considered in the study to be the control factors for the resistance of reinforcing bars in MPC to corrosion.

Keywords. MPC; rust; electrochemistry; pH; polarization curve.

1. Introduction

Magnesium phosphate cement (MPC) refers to a special sort of cementing material which boasts of more optimal performances over ordinary cementing materials. Blessed with various excellent characteristics, MPC shows better liquidity, faster setting and hardening, higher early strength, more favorable bond performance, better volume stability, higher abrasion resistance, and stronger salt corrosion resistance. Due to the feature of chemically bonded ceramics [1–8], it also serves as an ideal pavement patching material, extensively applied in the rapid repair of expressways, runways, and main roads. Moreover, its superb physiochemical properties make it widely applicable to military engineering, including first-aid repair and construction, the curing of harmful substances, and the transformation of solid waste into building materials. However, it is inevitable for the magnesium phosphate cement to have connection with the materials of reinforcing bars. Thus, a thorough investigation of its corrosion behaviors should be undertaken.

By virtue of its remarkable bonding with reinforcing bars, sound volume stability, and compact structure [9–19], MPC has been deemed as one special type of material able to well protect reinforcing bars by forming a compact protective layer similar to phosphate coating on the surface [20–26]. The hydration process leads to its transformation from weak acidity to neutrality and finally to alkalescence. Under weak acidic conditions, phosphating can hardly be achieved in the reinforcing bars at the beginning of hydration. It makes it impossible the formation of a stable protective layer with phosphate coating, thereupon. At the last stage of complete hydration, the pH reached about 10, creating a weak alkaline environment so that the formation can be avoided for the iron oxide passive coating layer [27–30]. Therefore, it is of considerable significance to explore the favorable conditions for MPC to save the reinforcing bars from corrosion.

This study aims to analyze the open circuit potential and polarization of reinforcing bars during corrosion and investigate their corrosion behaviors in the MPC system. Accordingly, a comparison of these performances was made between the MPC system and the ordinary cement by the electrochemical workstation. With regard to the

*For correspondence
Published online: 24 January 2020

reinforcing bars in MPC, their corrosion morphology at different ages of concrete was observed under an optical microscope, and also, the mechanism of resistance to corrosion was explored based on pH changes and polarization curve theory during the hydration of MPC.

2. Experiment

2.1 *Raw materials*

Supplied by Xuzhou Zhonglian Cement Corporation in China, the P.O 42.5 Portland cement with a specific surface area of 348 m^2/kg conformed to Chinese National Standard GB 175 (equivalent to European CEM I 42.5). Its chemical compositions are shown in table 1.

MPC was obtained by proportionally mixing magnesia oxide powder with $NH_4H_2PO_4$, and compound retarder in the laboratory. From the Huashan Plant in Shenyang Province, we purchased the dead burned magnesia powder with a specific surface area of 280 m^2/kg, calcined at >1700 °C, an average particle size of about 20μm, and a specific gravity of around 3.67 kg/m^{-3}. Its chemical compositions are listed in table 2.

Equipped with a maximum particle size of 700 μm and a purity of over 98%, industrial-grade $NH_4H_2PO_4$ worked as soluble phosphate. The compound retarder expressed as B [31] was prepared in the laboratory.

Holding a fineness modulus of 2.78 and a saturated surface dry specific gravity of 2760 kg/m^{-3}, the river sand was used as the fine aggregate and portable water for mixing.

2.2 *Mixing proportion*

By mixing the raw materials, cement mortar was prepared at a water-to-cement mass ratio (W/C) of 0.5. The dimension of specimens used in this research was 40 mm×40 mm×160 mm.

At a magnesia-to-phosphate molar ratio (M/P) of 4 and a phosphate paste-to-magnesia molar ratio (m_B/m_{MgO}) of 0.05, MPC mortar was prepared by mixing the raw materials. Here, the cement consisted of magnesia and NH4H2PO4, with the water-to-cement mass ratio (W/C) reaching 0.12. The dimension of MPC mortar specimens was 40 mm×40 mm×160 mm. The powdered materials made up from MgO, NH4H2PO4, and B were dry-mixed in a mixer pan for 3 min, which was added with 3% glacial acetic acid and mixed for another 1 min [31]. The grouping and mixture ratios are displayed in table 3.

Table 1. Chemical composition of Portland cement/(wt%).

SiO_2	Al_2O_3	Fe_2O_3	CaO	MgO	Na_2O	K_2O	SO_3	Loss
24.55	7.77	3.62	54.59	2.68	0.31	1.50	2.24	1.2

Table 2. Chemical composition of magnesium oxide powder/(wt%).

MgO	SiO_2	CaO	Loss
91.85	3.68	3.14	1.2

2.3 *Specimen preparation*

To ensure a full embedment in the cement and MPC during the corrosion tests, all embedded bars were composed of ribbed reinforcing bars in a length of 50 mm and diameter of 12 mm and glued together with PVC tubes. On each of the bars, one electrical wire was welded so as to take electrochemical measurements.

Reinforcing bars were implanted into the cement mortar test piece. The thickness of protective layers could reach up to 14 mm. A total of nine groups of the bars were utilized as test pieces in both the ordinary cement and the MPC. Then, they were immersed in a solution where the hydrochloric acid accounts for 1 mol/L for rapid corrosion test.

2.4 *Testing and characterization*

2.4a *pH test:* To study the influence of pH on reinforcing bar corrosion required an automatic temperature compensation pH tester to measure the pH values of MPC specimens prepared according to the specific ratio. The pH tester, with an accuracy of ±0.05Ph, was calibrated on the basis of JJF1547-2015 *Calibration Specification for On-line pH Meters*.

Throughout this process, the pH tester probe was kept embedded into the MPC slurry, and the pH values of MPC hardened specimens were recorded on the 1st d, 3rd d, 7th d, 28th d, 60th d, 180th d, 360th d, and 540th d.

2.4b *Compressive strength:* The mixed MPC slurry was mixed with standard sand at the ratio of 1:1.45 before being poured into the test model in size of 40 mm × 40 mm × 160 mm. After compaction, the mixture was vibrated 60 times on the rubber-sand jumping table. Then, the excess slurry was scraped off. Three hours later, the formed sample was demoulded. The temperature was controlled at

Table 3. Mix of MPC pastes.

Code name	$m_{MgO}/m_{NH_4H_2PO_4}$	m_B/m_{MgO}	m_L/m_{MPC}
M1	4	0	0.12
M2	4	3%	0.12
M3	4	5%	0.12
M4	4	10%	0.12

20 °C and relative humidity at 98%. The compression resistance of the sample was tested on the 1st d, 3rd d, 7th d and 28th d by WED100 electronic universal material testing machine.

2.4c *Electrochemical test*: The stationary potentiodynamic method, commonly applied to the investigation of corrosion in reinforcing bars, was employed in this study. To draw the polarization curve, an electrochemical workstation and corresponding testing software were adopted. A saturated copper sulfate electrode was taken as the reference electrode and sheet steel as the auxiliary electrode. Fitted to form the polarization curve, the measured $E - \lg I$ polarization values at different time nodes are available for the analysis of corrosion potential, E_{corr}, and the corrosion current, I_{corr}, two main assessment indices for reinforcement corrosion behavior evaluation [25].

2.4d *Micro-measurement*: X-ray fluorescence spectrometry analysis was conducted to determine the chemical composition of materials and element composition of test pieces after the corrosion of reinforcing bars.

3. Result and discussion

3.1 *Compressive strength*

Figure 1 shows the compressive strength development curve of MPC mortar with diverse composite retarders. According to the figure, the early strength of mortar specimens with different retarders undergoes a drastic increase. The strength of 1D and 3D exceeds 50 MPa while the strength of 7D increases by 20% compared with that of 1D. However, the growth of strength in the later phase slows down as the reaction proceeds.

Similar to that without retarder, the compressive strength of mortar with retarder presents a fast increase in the early stage and a slow growth in the later period, a pattern complying with the characteristics of high early strength of MPC. The 3-day strength without acetic acid was

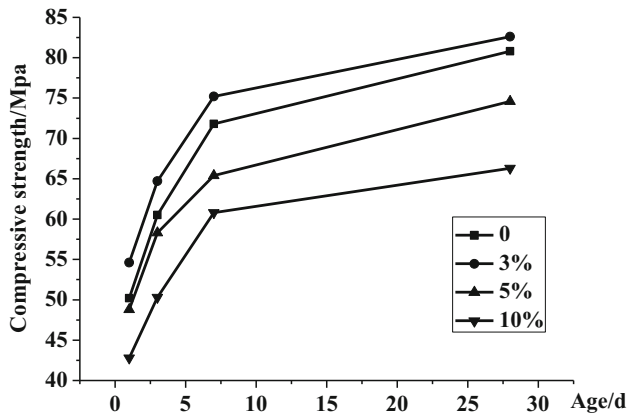

Figure 1. Development of compressive strength of MPC mortar.

61.5 MPa, and 65.7 MPa after acetic acid was added. The retarder played the role of both decelerating and early strengthening. Besides, the mix ratio of MPC mortar was M3 according to the change of strength and the fluidity of MPC mortar.

3.2 *pH*

Changes of pH in MPC system are reflected in table 4, suggesting the greater alterations of pH during setting and hardening. At the beginning of the setting, the slightly acidic environment in pH 6.7 was mainly controlled by ammonium dihydrogen phosphate. However, the dominating substance was being gradually consumed and thus led to the alkaline environment of pH 10.7. At this very moment, the system was largely manipulated by the hydration product, $MgNH_4PO_4{\cdot}6H_2O$. Finally, the MPC system was kept stable at the pH of about 10.8 after being completely hardened (table 5).corrosion induce the small

3.3 *Open circuit potential*

Open circuit potential (E_{corr}), also called (natural) corrosion potential, refers to the electrode potential when the current density reaches zero. It numerically equals the potential difference between the work and reference electrodes when the load is not applied. The open circuit potential could also be used to assess the probability of reinforcing bar rust.

Figure 2 demonstrates the changes in open circuit potential over time in the MPC and Portland cement. As found in the figure, the open circuit potential of the reinforcing bar electrode in Portland cement underwent subtle change in the first nine months, maintaining at -0.15 V(CSE), whereas it then reduced to -0.46 V(CSE) by the eighteenth month. This alteration indicated no rust taking place in the reinforcing bar in the Portland cement. Comparably, the open circuit potential of the reinforcing bar electrode in MPC remained low all the time, fluctuating around -0.1 V (CSE) and indicating little tendency to rust.

In conclusion, reinforcing bars in both MPC and Portland cement were not rusted according to the potential distribution and the corrosion degree with reference to the standard of China Metallurgy Ministry.

3.4 *Polarization curve*

The polarization curve represents the relation between the electrode potential and the exterior-measured current

Table 4. Changes of pH in MPC system.

Time (d)	1	3	7	28	60	180	360	540
pH	6.7	10.5	10.9	10.6	10.6	10.7	10.6	10.8

Table 5. The relationship between corrosion potential and corrosion of reinforcement.

E_{corr} (V)	E_{corr}>-0.25	-0.25<E_{corr}<-0.400	E_{corr}<-0.400
Degree of corrosion	No rust	May rust	Rust

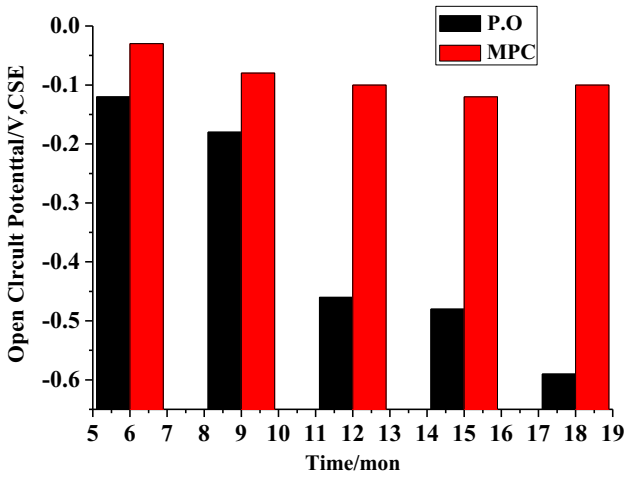

Figure 2. Open circuit potential changes of steel electrode system over time.

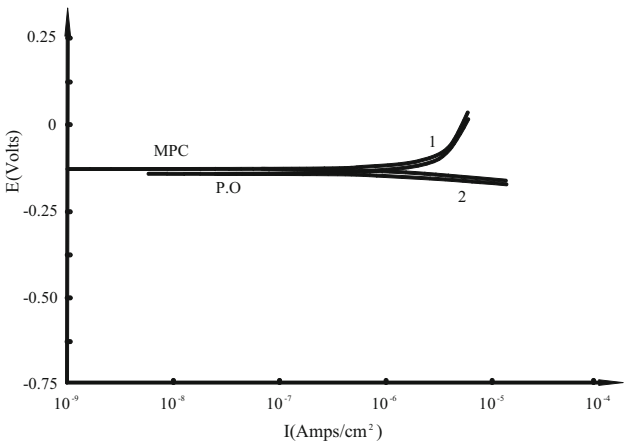

Figure 3. Polarization curves of reinforcing bars for 12 months.

density. In the coordinate, the electrode potential is expressed as E,or the polarization, ΔE, and the exterior measurement of the electrode current as I (or). Electrochemistry workstation or equivalent products can easily not only measure corrosion polarization but also calculate and analyze corresponding curves. Data in the weak polarization area has been processed on the basis of the corrosion electrochemistry principle. And the Gauss-Newton-Marquardt iteration was adopted for curve-fitting.

The polarization curve for a weak polarization area can be formulated as follows:

$$i = i_{corr}\left\{\exp\frac{E-E_0}{\beta_a} - \frac{\exp\frac{-(E-E_0)}{\beta_c}}{1-\frac{i_a}{i_L}\left[1-\exp\frac{-(E-E_0)}{\beta_c}\right]}\right\} \quad (1)$$

where i denotes the exterior measured polarization current density, i_{corr} stands for the corrosion current density, i_L refers to the limited diffusion current density, $\Delta E = E - E_0$ represents the polarization potential, and β_a and β_c are Tafel slopes of anode and cathode, respectively.

When$i_{corr} \le i_L$, Formula (1) can be simplified as:

$$i = i_{corr}\left\{\exp\frac{E-E_0}{\beta_a} - \exp\frac{-(E-E_0)}{\beta_c}\right\} \quad (2)$$

where i_{corr}, β_a, and β_c are three unknown parameters. Therefore, this formula is also named the three-parameter polarization curve formula.

3.4a 12-month corrosion test: Conditions with constant E and rapid corrosion induce the small slope of the polarization curve and an enormous current change. The electrochemical workstation records the change in the corresponding corrosion current in the course of the electrokinetic potential linearly from -0.03 V to +0.03 V. The corrosion potential E_{corr} (Points 1 and 2) has measured the 12-month polarization curves of the reinforcing bars in MPC and Portland cement, according to figure 3.

The slopes for Portland cement and MPC intertwine, indicating an equal resistance in these two types of cement. Moreover, they also shared similar values in currents, as depicted in table 6. According to the corrosion current appraisal parameters, no corrosion marks were observed on the reinforcing bars in Portland cement or MPC.

3.4b 18-month corrosion test: Figure 4 displays the 18-month polarization curves for two groups of reinforcing bars in Portland cement and MPC at the corrosion potential E_{corr} (Points 1 and 2 in the figure). It manifests the similar curve slopes for the bars in Portland cement and magnesium phosphate cement. In other words, bars in Portland cement and MPC shared similar polarization resistance. According to the measured corrosion current in table 7, the current of the former bore resemblance to that of the latter. Besides, corrosion marks were not found in the reinforcing

Table 6. Processing results 12 months of reinforcement corrosion weak polarization region data.

Number	Fitting accuracy	b_a/mV	b_c/mV	I_{corr}/(A)
MPC	1.0	422.86	44.56	2.76×10^{-3}
P.O	1.0	715.89	42.80	2.90×10^{-3}

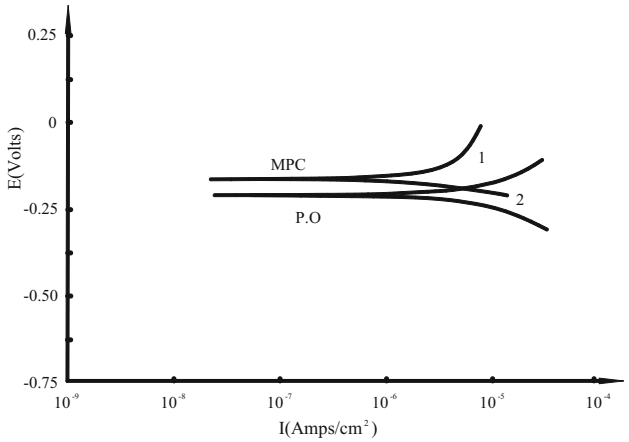

Figure 4. Polarization curves of reinforcing bars for 18 months.

Table 7. Processing results 18 months of reinforcement corrosion weak polarization region data.

Number	Fitting accuracy	b_a/mV	b_c/mV	I_{corr}/(A)
MPC	1.0	83.18	77.79	4.28×10^{-3}
P.O	1.0	135.72	58.74	2.15×10^{-3}

bars in both cement, as perceived from the corrosion current appraisal parameters.

3.5 *Reinforcing bar rust pattern in different periods*

Figure 5 depicts the 12-month longitudinal section morphology of reinforcing bar corrosion in the ordinary cement. Here, a large area of corrosion could be found on the bar surface, along with obvious corrosion pits. In addition, a distinct rust-overflow phenomenon could also be observed in both terminals of concrete, whereas uniform reinforcing bar corrosion could be perceived inside the concrete. In contrast, a large area of continuous corrosion appears on the reinforcing bar surface in 18 months, and almost the entire test piece is corroded.

Figure 6 exhibits the rust pattern of the reinforcing bar in MPC in a longitudinal section. By the 12th month, the reinforcing bar in the MPC has presented a smooth and

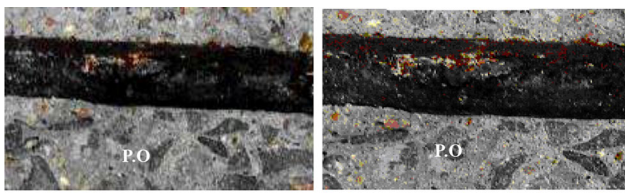

(a) 12 months **(b) 18 months**

Figure 5. Corrosion morphology of reinforced concrete.

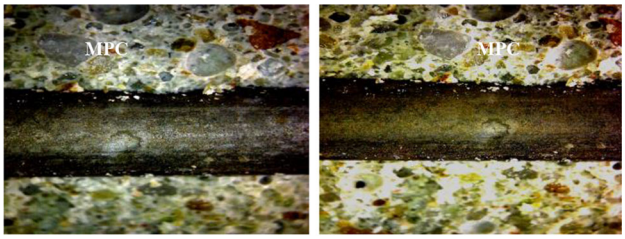

(a) 12 months **(b) 18 months**

Figure 6. Corrosion morphology of MPC.

clean surface, similar to that without cement. By the 18th month, the surface has never displayed neither a large area of rust nor overt rust pits. At the same time, there has been no rust overflow on two ends of the concrete. Without the occurrence of continuous rust, the whole single bar remains intact.

Therefore, it can be concluded that the reinforcing bar in MPC is immune to corrosion judging by its even surface.

4. Mechanism analysis

4.1 *Causes of corrosion*

A positive shift could be observed during the negative shift of corrosion potential of ordinary cement test piece within test time. It reveals a high vulnerability of ordinary cement reinforcing bar to corrosion. The corrosion rate of ordinary cement reinforcing bar initially went up, then maintained at a higher level, and subsequently dropped. The corrosion layer formed early partially hindered the generation of new corrosion which is inevitable, however. Moreover, increasingly serious corrosion would also take place afterwards.

The negative shift of MPC reinforcing bar corrosion potential within test time clarifies the resistance of MPC to corrosion. The corrosion rate of MPC reinforcing bar, generally keeping extremely low, fluctuates dramatically before the first 12 months and then maintains at a relatively stable level later. This implies an erratic resistance of MPC to corrosion in the first 12 months. MPC was slightly alkaline, and its cement mortar filtrate fluctuated around pH 10.0. Overall, the reinforcing bar in MPC concrete could hardly be corroded.

4.2 *Influence of pH on reinforcing bar rust in MPC*

A passivating film is formed on the surface of the reinforcing bar, whose anodic and cathodal polarization curves of the reinforcing bar are depicted in figure 7. Curve A denotes the anodic polarization curve of the reinforcing bar in concrete. It could be divided into three areas, namely, the

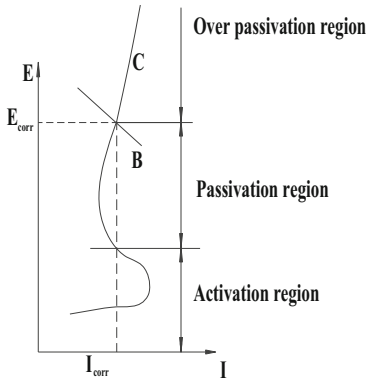

Figure 7. Evans diagram of passive steel corrosion in alkaline environment.

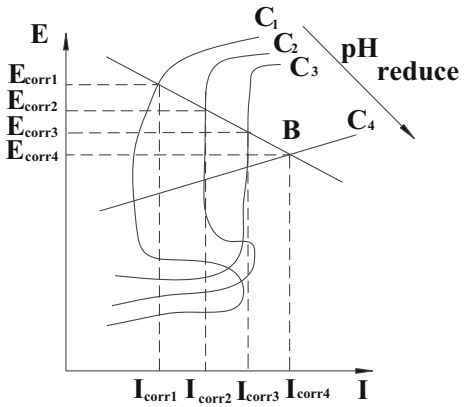

Figure 8. Evans diagram of effect of pH on reinforcing bar corrosion.

active area, the passivation area, and the over-passivation area. Curve C represents the cathodic polarization curve of the oxidation–reduction reaction. At the junction of curves A and C, rates of anode and cathode reactions achieve balance. The potential and current corresponding to the junction are expressed as E_{corr} and I_{corr}, respectively. The typically stable state of the reinforcing bar in concrete is attributed to the passivation area of the anode curve shared by both anode and cathode curves. The I_{corr} is small and negligible. The rust course of the reinforcing bar in Portland cement could be separated into three areas while that in the MPC only occurs in the passivation area.

The reinforcement in MPC starts to be activated and the corrosion behavior continues. Because the hydration reaction of MPC matrix is still in progress and equipped with excellent volume stability and cohesion with the reinforcement, the corrosion products formed on the surface of the electrodes are difficult to follow up reactions and transfers. Thus, they can only produce a dense mixed layer on the bonding layer. Consequently, an augment is rendered in the resistance of the bonding layer and in the polarization resistance of the reinforcing bar.

The original environment of MPC system is acidic. And it is in such environment that the chemical reaction film is formed on the surface of steel bars. Contrary to the stable state of the bonding interface, the chemical reaction film is erratic. The intensification of the corrosive environment results in the destruction of the film and the slowdown of the corrosion reaction on the surface of steel bars. On account of the difficulty in developing the rust product during transferring, it can only react with MPC. When the bonding layer is penetrated by harmful ions, the surface charge and material transfer resistance of the steel bar and the polarization resistance lessen irreversibly. When the MPC system maintains a high basicity, it is difficult to form chemical reaction films on the surface of steel bars. Additionally, slow corrosion reaction products on the surface of steel bar combine with bonding layer, and the polarization resistance value grows gradually.

Therefore, it is challenging for steel bars to form a stable protective film on the surface of the MPC system. The protective effect on steel bars is mainly embodied by the excellent chemical ceramic properties of the matrix of MPC, stable volume, and proper bonding with steel bars. The protective effect of MPC on steel bars only works physically, that is, under whose protection the corrosion reaction always exists. Moreover, the corrosion proceeds at an unprecedentedly speed.

Figure 8 illustrates the change in the corrosion potential and corrosion current caused by the pH change in MPC. Curves A and C respectively represent the anodic and cathodic polarization curves of the reinforcing bar with various pH. The decline in the pH on the surface of the reinforcing bar leads to the reduction of the passivation area of the anodic polarization curve and the transformation of the anodic polarization curve from A1 to A3. When the pH on the reinforcing bar surface is equal to the value of the critical corrosion, the passivation area disappears (as shown in figure A4) from the anodic polarization curve. As the pH rises on the reinforcing bar surface, the corrosion potential elevates ($E_{corr4}<E_{corr3}<E_{corr2}<E_{corr1}$), whereas the corresponding corrosion current diminishes ($I_{corr4}>I_{corr3}>I_{corr2}>I_{corr1}$). The pH of MPC system remains stable at the value of 10.0 within the test time. Moreover, the reinforcing bar is in the passive region to withstand weak corrosion.

4.3 *Corrosion products of reinforcing bar*

Reinforcing bar in the ordinary cement is seriously corroded while that in the MPC is slightly affected. In this context, EDS analysis on the reinforcing bar surface will favor the analysis of the corrosion behavior of reinforcing bar.

The immersion of chloride ion onto reinforcing bar surface accelerates the corrosion on the surface of the latter, giving rise to the corrosion of the reinforcing bar in the

Table 8. EDS of steel in MPC before and after test (wt/%).

Before test		After test					
C	Fe	C	Fe	P	Mg	N	O
5.8	94.2	6.78	53.07	28.92	24.25	7.35	0.37

ordinary cement. Studies have demonstrated that the corrosion products generated by the reinforcing bars in ordinary cement mainly encompass $Fe(OH)_3$, FeOOH (reddish brown rust) and Fe_2O_3 [23–25]. As described in figure 5, there are blocky compact products in reddish brown. The exposed corrosion layer of reinforcing bar is mostly irregular in structure and characterized as an unevenly distributed band. Concurrently, the layer also features tough surface and strong stereoscopic impression.

Furthermore, table 8 suggests that the MPC-made reinforcing bar consists of two elements, C and Fe, before the test. In comparison, extra elements of Mg, N, P and O are produced on the surface of the bar after the test. Thus, it could be inferred that long-time immersion contributed to the movement of Mg, N, P, and O elements, in addition to iron oxides, from MPC onto the surface of MPC reinforcing bar. The corrosion layer on MPC reinforcing bar surface probably resulted from the interpenetration of soluble components in the reinforcing bar and surrounding cement mortar, thereby forming the phosphate metal complex.

5. Conclusions

(1) The reinforcing bar corrosion behavior in MPC was distinctive compared to that in Portland cement. The analysis of the corrosion potential, corrosion current, and polarization curves proved the strong corrosion resistance of reinforcing bars in the MPC.

(2) Magnesium cement reinforced concrete is oxidized and corroded in a solution with chloride ion concentration of 3 mol/L. The corrosion products show multi-layers (loose and massive rust layer with weak external protective effect; internal rust layer has a certain effect on inhibiting metal corrosion, and the rust layer is relatively uniform). When electrochemical tests are carried out, because of the influence of corrosion products covered on the surface, the corrosion mass loss of reinforcing steel bars and the corrosion current density decrease sharply in the solution with chloride concentration of 3 mol/L, and the corrosion rate slows down. The major reason is that when concrete is immersed in magnesium chloride solution, water and corrosive chloride ions penetrate through concrete pore or microcrack. The acceleration of the corrosion of the steel bar and the corrosion rate is caused by the invasion of the chloride ions into the environment where the steel bar is located to form a salt concentration cell, and chloride ions depolarize the steel bar, which brings about the destruction of the local coating on the surface of the coated steel bar and the occurrence of pitting corrosion.

(3) The protective mechanism of MPC system for reinforcing bars can be summed up as the constant corrosion reaction on the surface of reinforcing bars. Because of the stability of MPC matrix and the formation of a dense bonding layer at the interface of reinforcing bars, it is difficult for the corrosion products to transfer to the outside, and only a dense compound bonding layer can be formed at the interface bonding layer in the presence of water, which prevents the further corrosion reaction over time. After chloride ion plasma penetrates the matrix and bond layer, the damage to steel bars lessens the resistance of charge and material transfer on the surface of steel bars, and the corrosion reaction is likely to continue and advance. Only when the resistance of matrix and bonding layer to ion and charge transfer weakens to a certain extent, the steel bar electrodes in MPC may be corroded massively and dramatically.

Acknowledgements

The authors would like to express their gratitude to Science and Technology Program of Henan Province of China (182102210418), and Key scientific research projects of universities in Henan (19B560004;20B560010), and National Natural Science Foundation of China (51972337), and Funding for the high-level scientific research team of Kaifeng University, and Funded by the science and technology platform of Kaifeng University collaborative innovation center for new energy-saving building materials.

References

[1] Jiang H and Changming C 2010 Influence of admixtures on the dissolution rate of chloride ion in magnesia cement. *Journal of Wuhan University of Technology* 32(18): 37–40

[2] Yang J M, Shi C, Chang Y, Yang N 2013 Hydration and hardening characteristics of magnesium potassium phosphate cement paste containing composite retarders. *Journal of Building Materials* 1: 43–49

[3] Li Y and Chen B 2003 Factors that affect the properties of magnesium phosphate cement. *Construction and Building Materials* 47: 977–983

[4] Soudee E and Pera J 2002 Influence of magnesia surface on the setting time of magnesia-phosphate cement. *Cement and Concrete Research* 32(1): 153–157

[5] Mestres G and Ginebra M 2011 Novel magnesium phosphate cements with high early strength and antibacterial properties. *Acta Biomaterialia* 7(4): 1853–1861

[6] Sarkar A K 1990 Phosphate cement-based fast-setting binders. *American Ceramic Society Bulletin* 69(2): 234–238
[7] Brantschen F, Faria D M V and Ruiz M F 2016 Bond behaviour of straight, hooked, U-shaped and headed bars in cracked concrete. *Structural Concrete* 17(5): 799–810
[8] Zhu C, Chang X, Men Y and Luo X 2015 Modeling of grout crack of rockbolt grouted system. *International Journal of Mining Science and Technology* 25: 73–77
[9] De Villiers J P, van Zijl G P A G and van Rooyen A S 2017 Bond of deformed steel reinforcement in lightweight foamed concrete. *Structural Concrete* 18(3): 496–506
[10] Prince M J R and Singh B 2015 Bond behaviour of normal- and high-strength recycled aggregate concrete. *Structural Concrete* 16(1): 56–70
[11] Seehra S, Gupta S and Kumar S 1993 Rapid setting magnesium phosphate cement for quick repair of concrete pavements-characterisation and durability aspects. *Cement and Concrete Research* 23(2): 254–266
[12] Prosen E M 1939 *Refractory materials for use in making dental casting*. US Patent: 2, 152, 152
[13] Subei O, Lianguo W, Peipei W, Zhansheng W, Huang J and Donglei J 2013 Numerical analysis of seepage flow characteristic of collapse column under the influence of mining. *International Journal of Mining Science and Technology* (2): 8–11
[14] Earnshaw R 1960 Investments for casting cobalt-chromium alloys, part I. *Br. Dent. J.* (108): 389–396
[15] Earnshaw R 1960 Investments for casting cobalt-chromium alloys, part II. *Br. Dent. J.* 108: 429–440
[16] Ma H and Xu B 2014 Potential to design magnesium potassium phosphate cement paste based on an optimal magnesia-to-phosphate ratio. *Materials and Design* 118:81–88
[17] Lahalle H, Coumes C C D, Mesbah A, Lambertin D, Cannes C, Delpech S, Gauffinet S 2017 Investigation of magnesium phosphate cement hydration in diluted suspension and its retardation by boric acid. *Cement and Concrete Research* 87: 77–86
[18] Viani A, Peréz-Estébanez M, Pollastri S, Gualtieri A F 2016 In situ synchrotron powder diffraction study of the setting reaction kinetics of magnesium-potassium phosphate cements. *Cement and Concrete Research* 79: 344–352
[19] You C, Qian J, Qian J, Wang H, Wang Q and Ye, Z 2015 Effect of early hydration temperature on hydration product and strength development of magnesium phosphate cement (MPC). *Cement and Concrete Research*, 78, Part B,:179–189
[20] Gardner L, Bernal S, Walling S, Corkhill C, Provis J and Hyatt N 2015 Characterisation of magnesium potassium phosphate cements blended with fly ash and ground granulated blast furnace slag. *Cement and Concrete Research* 74: 78–87
[21] Xu B, Ma H and Li Z 2015 Influence of magnesia-to-phosphate molar ratio on microstructures, mechanical properties and thermal conductivity of magnesium potassium phosphate cement paste with large water-to-solid ratio. *Cement and Concrete Research* 68: 1–9
[22] Ma H, Xu B, Liu J, Pei H and Li Z 2014 Effects of water content, magnesia-to-phosphate molar ratio and age on pore structure, strength and permeability of magnesium potassium phosphate cement paste. *Materials and Design* 64: 497–502
[23] Ma H, Xu B and Li Z 2014 Magnesium potassium phosphate cement paste: degree of reaction, porosity and pore structure. *Cement and Concrete Research* 65: 96–104
[24] Shi C, Yang J, Yang N and Chang Y 2015 Effect of waterglass on water stability of potassium magnesium phosphate cement paste. *Cement and Concrete Composites* 53:83–87
[25] Ji YS, Zhao W and Zhou M 2013 Corrosion current distribution of macro cell and microcell of reinforcing bar in concrete exposed to chloride environments. *Construction and Building Materials* 47:104–110
[26] Yang Q, Zhang S and Wu X 2002 Deicer-scaling resistance of phosphate cement-based binder for rapid repair of concrete. *Cement and Concrete Research* 32(1):165–168
[27] Yang Q, Zhu B, Zhang S, Wu X 2000 Properties and applications of magnesia-phosphate cement mortar for rapid repair of concrete. *Cement and Concrete Research* 30(11): 1807–1813
[28] Ding Z 2005 *Research of Magnesium Phosphosilicate Cement*. Hongkong Universityof science and technology, Doctor[D], Hongkong: Hongkong University of science and technology pp 100–120
[29] Zhu D and Zongjin L 2006 High early strength magnesium phosphosilicate cement (in Chinese). *Chinese Jounral of Materials Research* 20(2): 141–147
[30] Ghirian A and Fall M 2016 Strength evolution and deformation behaviour of cemented paste backfill at early ages: Effect of curing stress, filling strategy and drainage. *International Journal of Mining Science and Technology* 26(5): 809–817
[31] Jun L, Yong-sheng J and Guodong H 2017 Retardation and reaction mechanisms of magnesium phosphate cement mixed with glacial acetic acid. *RSC Advances* 7(74): 46852–46857